

Downregulation of p16^{ink4a} inhibits cell proliferation and induces G1 cell cycle arrest in cervical cancer cells

CHU-YUE ZHANG, WEI BAO and LI-HUA WANG

Department of Obstetrics and Gynecology, International Peace Maternity and Child Health Hospital of China Welfare Institute, Shanghai Jiao Tong University School of Medicine, Shanghai 200030, P.R. China

Received December 17, 2013; Accepted March 28, 2014

DOI: 10.3892/ijmm.2014.1731

Abstract. Studies have suggested that p16^{ink4a} may be a surrogate biomarker for the diagnosis of cervical cancer; however, the function of p16^{ink4a} in human cervical cancer cells remains largely unknown. Therefore, in this study, we aimed to investigate the role of p16^{ink4a} in human cervical cancer cells. Immunocytochemistry was used to examine invasive squamous cell carcinoma and its precancerous lesions. p16^{ink4a}-siRNA was transfected into SiHa and HeLa cells to deplete its expression. The cellular levels of p16^{ink4a} mRNA and protein were detected by qRT-PCR and western blot analysis. Proliferation rates were assessed by methyl thiazolyl tetrazolium (MTT) and plate colony formation assays. Cellular migration and invasion ability were assessed by a wound healing assay and Transwell assay. Cellular apoptosis and the cell cycle were measured by flow cytometry. The protein levels of retinoblastoma (Rb), phosphorylated Rb (phospho-Rb), cyclin D1 and caspase-3 were determined by western blot analysis. The results revealed that p16^{ink4a} was overexpressed in the cervical cancer and precancerous lesions (P<0.05). The downregulation of p16^{ink4a} in the SiHa and HeLa cells inhibited their proliferation, migration and invasion. In the SiHa cells, p16^{ink4a}-siRNA also induced G1 cell cycle arrest and apoptosis. Western blot analysis revealed that the downregulation of p16^{ink4a} in the SiHa cells markedly induced caspase-3

activation and decreased cyclin D1 expression. These data suggest that the overexpression of p16^{ink4a} appears to be useful in monitoring cervical precancerous lesions, which supports that the hypothesis that p16^{ink4a} is a surrogate biomarker for the diagnosis of cervical cancer. The therapeutic targeting of overexpressed p16^{ink4a} in the p16^{ink4a}-cyclin-Rb pathway may be a useful strategy in the treatment of cervical cancer.

Introduction

Cervical cancer is the third most common cancer worldwide, with an annual incidence of 530,000 cases, and an estimated 250,000 deaths (1). Cervical cancer is also the second leading cause of mortality in women between the ages of 20 and 39 (2). The cervical cytology screening of specimens for oncogenic human papilloma virus (HPV) has led to a decrease in the incidence of cervical cancer in most developed countries by 70% over the past 50 years (3,4). However, developing countries still face a serious challenge (5). In China, the incidence of cervical cancer has increased in recent years, particularly in the younger generation (6,7). Current therapeutic approaches are associated with limited success. In advanced disease, chemotherapy remains the standard of care (8). To improve clinical outcomes, it is imperative to investigate the molecular pathways underlying the pathophysiology of the disease, and to identify novel diagnostic and therapeutic targets.

p16^{ink4a}, a tumor suppressor protein, is an inhibitor of cyclin-dependent kinase (CDK)4/6 and is involved in cell cycle regulation mediated by the retinoblastoma (Rb) gene complex. It has been reported that p16^{ink4a} is mutated and deleted in various human tumors (9-12). However, it is overexpressed in cervical cancer and its precancerous lesions. The levels of p16^{ink4a} protein are generally low in normal cervical cells, but are upregulated in HPV-infected cervical cells due to the inactivation of the Rb complex by the HPV E7 oncoprotein (13). Studies have suggested that the overexpression of p16^{ink4a} correlates with the degree of cervical neoplasia (14,15), which may improve the histological diagnosis of cervical lesions. However, no direct evidence is available to indicate that the expression of p16^{ink4a} affects cervical cancer. Therefore, in this study, we investigated the role of p16^{ink4a} overexpression in cervical cancer and the associated cellular pathophysiology.

In the present study, we explored the role of p16^{ink4a} in the pathogenesis of cervical cancer and investigated the effects of

Correspondence to: Professor Li-Hua Wang, International Peace Maternity and Child Health Hospital of China Welfare Institute, Shanghai Jiao Tong University School of Medicine, 910 Hengshan Road, Shanghai 200030, P.R. China
E-mail: drwanglh0420@163.com

Abbreviations: ICC, immunocytochemistry; MTT, methyl-thiazolyl tetrazolium; HPV, human papilloma virus; CIN, cervical intraepithelial neoplasia; ISCC, invasive squamous cell carcinoma; HSIL, high-grade squamous intraepithelial lesion; LSIL, low-grade squamous intraepithelial lesion; ASCUS, atypical squamous cells of undetermined significance

Key words: p16^{ink4a}, cervical intraepithelial neoplasia, cervical cancer, proliferation, G1 cell cycle arrest, apoptosis

the downregulation of p16^{ink4a} on cervical cancer cell proliferation, apoptosis and cell cycle arrest.

Materials and methods

Sample collection and handling. Residues of 149 ThinPrep-processed cervical cytology samples were collected from the International Peace Maternity and Child Hospital, Affiliated to Shanghai Jiao Tong University (Shanghai, China), from February 2010 to February 2011. The age of the patients was between 22 and 60 years (mean age, 35 years); none of the patients were pregnant, and none had a history of cervical surgery or pelvic radiation therapy. The samples included 20 cases of high-grade squamous intraepithelial lesions (HSILs), 42 cases of low-grade squamous intraepithelial lesions (LSILs), 50 cases of atypical squamous cells of undetermined significance (ASCUS), 17 cases of negative samples and 20 cases of invasive squamous cell carcinoma (ISCC). The diagnosis and histological classification of the cervical cancer samples were carried out according to the criteria proposed by the International Federation of Gynecology and Obstetrics (FIGO). The patients, including 35/50 (70%) ASCUS cases and 36/42 (86%) of the LSIL cases were subjected to cytological and histological analyses within 2 years of the initial diagnosis. The use of cytological residues was approved by the Human Investigation Ethical Committee of the International Peace Maternity and Child Health Hospital Affiliated to Shanghai Jiao Tong University. The residues of the cervical cytological samples were centrifuged at 1,500 rpm for 3 min, followed by incubation with agarose solution (agarose:H₂O, 1 g:50 ml). Paraffin sections (5-mm³-thick) were obtained after cooling down the samples.

Immunocytochemistry (ICC). Thin-layer cytology slides were dried overnight in an oven at 37°C. Antigen retrieval was performed by heating the immersed slides in 10 mM sodium citrate buffer, pH 6.0, at 951°C in a microwave oven for 15 min. Endogenous peroxidase was blocked by treatment with 3% H₂O₂ in methanol. Rabbit monoclonal antihuman p16^{ink4a} (Epitomics, Burlingame, CA, USA) antibodies were used at a dilution of 1:1,000. Antibody binding was detected using EnVision reagents (Boster Bio-Engineering Co., Ltd., Wuhan, China), according to the manufacturer's instructions. A light hematoxylin counterstain was used. The primary antibody was replaced with preimmune IgG serum and used as a negative control. HeLa cells were used as the positive control. The experimental conditions were uniform for all the samples. Morphological criteria based on a modified scoring system described in the study by Wentzensen *et al* (16) were used for the assessment of the immunoreactivity of the cells for p16^{ink4a}. More than 10 epithelial groups were assessed in each slide with the highest immunoreactivity. Cells with atypical cytological features were evaluated for immunoreactivity and an index of 0–4 was obtained. The immunoreactivity for p16^{ink4a} in the samples was evaluated by 2 of the authors. Cases with discrepancy in scoring were resolved under a multihead microscope (Zeiss Axioskop 40; Zeiss, Oberkochen, Germany). The specific cytological diagnosis of the samples was disclosed after the scoring.

Cell culture. Human cervical cancer cell lines (SiHa and Hela) were obtained from the Committee on Type Culture

Collection of the Chinese Academy of Sciences (Shanghai, China). Cells were maintained at 37°C in a humidified atmosphere containing 5% CO₂ in Dulbecco's modified Eagle's medium (DMEM)/F12 (11030; Gibco, Auckland, New Zealand) supplemented with 10% fetal bovine serum (FBS) (16000-44; Gibco, Carlsbad, CA, USA).

Preparation and transfection of siRNA targeting p16^{ink4a}. In order to inhibit the expression of endogenous p16^{ink4a}, we designed and prepared an HPLC-purified p16^{ink4a}-siRNA, based on the p16^{ink4a} gene sequence. A scrambled siRNA with no homology to any known human mRNA was used as a negative control. siRNA oligonucleotide duplexes were synthesized by Shanghai GenePharma Co., Ltd. (Shanghai, China). The sequences of the p16^{ink4a}-siRNA oligonucleotides were as follows: forward, 5'-CGCACCGAAUAGUUACGG UTT-3' and reverse, 5'-ACCGUAACUAUUCGGUGCGTT-3'. The cells were seeded in 12-well plates till they reached 70–80% confluence and were grown overnight prior to transfection. The transfection of the SiHa and Hela cells with the p16^{ink4a}-siRNA or the non-target control-siRNA was accomplished using the Lipofectamine 2000 transfection reagent (Invitrogen, Carlsbad, CA, USA), according to the manufacturer's instructions. The experimental groups were classified into the p16^{ink4a}-siRNA, the control-siRNA and the untreated group.

RNA extraction and quantitative RT-PCR (qRT-PCR). Total RNA was isolated using TRIzol reagent (Invitrogen Life Technologies; Shanghai, China) and reverse transcribed using a reverse transcriptase kit (Takara Biotechnology, Dalian, China). Gene expression detection was performed using SYBR-Green Master mix (Takara) on using an ABI Prism 700 thermal cycler (Applied Biosystems, Foster City, CA, USA) according to the manufacturer's instructions. Gene expression was calculated using the 2^{-ΔΔCt} formula. The primer sequences used were as follows: p16^{ink4a} forward, 5'-CTTCTGGACACGCTGGT-3' and reverse, 5'-ATCTATGCGGGCATGGTTACT-3'; and β-actin forward, 5'-CAGCCATGTACGTTGCTATCCAGG-3' and reverse, 5'-AGGTCCAGACGCAGGATGGCATG-3'. Duplicate reactions were performed for each sample, and the same experiment was repeated 3 times, with β-actin as a reference gene.

Western blot analysis. Cells were grown in 10-cm dishes. After 2 rinses in ice-cold PBS, the cells were physically harvested and lysed in ice-cold HNTG buffer [50 mmol/l HEPES (pH 7.5), 150 mmol/l NaCl, 10% glycerol, 1% Triton X-100, 1.5 mmol/l MgCl₂, 1 mmol/l EDTA, 10 mmol/l sodium PPI, 100 μmol/l sodium orthovanadate, 100 mmol/l NaF, 10 μg/ml aprotinin, 10 μg/ml leupeptin and 1 mmol/l PMSF] on ice for 30 min. The total protein content was determined using the BCA protein assay kit (Pierce, Rockford, IL, USA). Protein samples (20 μg) were subsequently separated on 12% sodium dodecyl sulfate polyacrylamide electrophoresis (SDS-PAGE) gels and electrotransferred onto PVDF membranes. The membranes were blocked and then probed with antibodies against p16^{ink4a} (1:500 dilution), Rb (1:1,000 dilution) (both from Epitomics), phosphorylated Rb (phospho-Rb; 1:1,000 dilution; Cell Signaling Technology, Danvers, MA, USA), cyclin D1 (1:10,000 dilution; Epitomics), caspase-3 (1:6,000

dilution; Cell Signaling Technology). Data were normalized to β -actin expression (1:1,000; Proteintech Group, Inc., Chicago, IL, USA) by densitometry. Statistical data from at least 3 experiments were analyzed for additional validation.

Cell proliferation assay. The cells were seeded into 96-well plates at 2×10^5 cells/ml and cultured in DMEM/Ham's F12 medium supplemented with 10% FBS for 1-5 days. Cell growth was documented every 24 h via a colorimetric assay using a 3-(4,5-dimethylthiazol-2-yl)-2,5-diphenyltetrazolium bromide (MTT) assay (Sigma, St. Louis, MO, USA). The absorbance was determined at 490 nm using a SpectraMax 190 microplate reader (Molecular Devices, Sunnyvale, CA, USA). The control samples were treated with the vehicle (0.1% DMSO or ethanol in DMEM/Ham's F12 culture medium). In each individual experiment, proliferation was determined in triplicate, and the overall experiment was repeated at least 3 times.

Wound healing assay. For wound healing experiments, cells (5×10^6 /well) were seeded in 6-well plates and allowed to adhere for 24 h. Cell monolayers were scarred with a sterile micropipette tip and incubated in serum-free medium for 24 h. Three defined areas of each sample were monitored, and photographed at 0, 6, 12 and 24 h. The migration index was calculated from the distance traveled by the cell monolayer relative to the gap created with the pipette tip at 0 h, for the untreated, control-siRNA- or the p16^{ink4a}-siRNA-treated cells, as previously described (17).

Transwell migration assay. Experiments were performed using 6.5-mm Transwell chambers equipped with 8.0 μ m pore-size polycarbonate membranes (Corning, Inc., Glendale, AZ, USA). Cells (1×10^5) were added to the top section of a Boyden chamber apparatus in 150 ml serum-free DMEM medium. Subsequently, 600 ml complete medium were added to the lower chamber. Following 10 h of incubation, the cells that had attached to the underside of the membrane were fixed with 4% paraformaldehyde. The cells were stained with 5% crystal violet and counted at 200-fold magnification. The migration assay was repeated at least 3 times.

Transwell invasion assay. The upper chambers were first coated with 40 ml of Matrigel at a 1:3 dilution (BD Biosciences, Franklin Lakes, NJ, USA) and incubated at 37°C for 2 h, followed by the addition of 1×10^5 cells to the top section of a Boyden chamber apparatus in 150 ml serum-free DMEM medium and 600 ml complete medium to the lower chamber. Following 24 h of incubation, the cells that had attached to the underside of the membrane were fixed with 4% paraformaldehyde. The cells were stained with 5% crystal violet and counted at 200-fold magnification. The invasion assay was repeated at least 3 times.

Colony formation assay. Approximately 1×10^3 cells were seeded into each well of a 6-well culture plate and incubated for 14 days at 37°C, followed by washing in PBS twice and staining with crystal violet. The number of colonies containing ≥ 50 cells was counted under a light microscope, and calculated as follows: Plate clone formation efficiency (%) = (number of

colonies/number of cells inoculated) $\times 100$. Each experiment was performed in triplicate.

Apoptosis and cell cycle analysis. The cells were harvested and subjected to dual staining with Annexin V and propidium iodide (PI) using an Annexin V-PI Apoptosis Detection kit (KeyGEN Biotech Co., Ltd., Nanjing, China). Separately, the cells were harvested and subjected to staining with PI using a Cell Cycle Detection kit (KeyGEN Biotech Co.). The cells were treated according to the manufacturer's instructions. The resulting fluorescence intensities were measured by flow cytometry using a Beckman Coulter FC 500 flow cytometer (Beckman Coulter, Inc., Brea, CA, USA). Experiments were performed in triplicate and reproducibility was confirmed in 3 independent experiments.

Statistical analysis. All statistical analyses were performed using the Statistical Package for the Social Sciences (SPSS) software version 17.0 (SPSS, Inc., Chicago, IL, USA). The significance of the differences in p16^{ink4a} expression among all cervical cytology diagnostic categories was examined using a non-parametric Kruskal-Wallis H test and an χ^2 test. The significance of the differences in p16^{ink4a} expression between any 2 diagnostic groups was analyzed by the Student-Newman-Keuls (SNK) test. Data are presented as the means \pm standard deviations (SD). Data were assessed using a Student's t-test or one-way ANOVA analysis for multiple comparisons. Values of $P < 0.05$ or $P < 0.01$ or $P < 0.001$ were considered to indicate statistically significant differences. All experiments were carried out in triplicate and repeated at least 3 times.

Results

p16^{ink4a} is overexpressed in cervical intraepithelial neoplasia (CIN) and cervical cancer. The immunoreactivity of p16^{ink4a} was predominantly localized in the nuclei, although a weak cytoplasmic expression was observed focally and occasionally (Fig. 1A). The normal squamous cells were negative for p16^{ink4a}. The focal weak to moderate immunoreactivity of p16^{ink4a} was noted in the ASCUS and LSIL samples. The HSIL and ISCC samples were often strongly positive for p16^{ink4a}. A comparison of the p16^{ink4a} index in the different categories of cervical cytology diagnosis is summarized in Fig. 1B. A statistically significant difference was observed in the p16^{ink4a} index among the different diagnostic categories ($P < 0.001$, Kruskal-Wallis test). The ASCUS and LSIL samples showed a significantly higher p16^{ink4a} index ($P < 0.05$, SNK test) compared with the negative cervical cells, although no significant difference in the p16^{ink4a} index was noted between the ASCUS and LSIL categories. No significant difference was observed in the p16^{ink4a} index between the HSIL and ISCC samples. However, the HSIL samples showed a significantly higher p16^{ink4a} index than the ASCUS and LSIL samples ($P < 0.05$, SNK test).

To determine whether p16^{ink4a} enables the evaluation of the likelihood of progression in a particular CIN, we compared the p16^{ink4a} expression of the ASCUS and LSIL cases manifesting different pathologies. The cytology and histological follow-up data of the patients within 2 years after the initial diagnosis were available for 35/50 (70%) of the ASCUS and 36/42 (86%) of the LSIL cases (Table I). Among the ASCUS

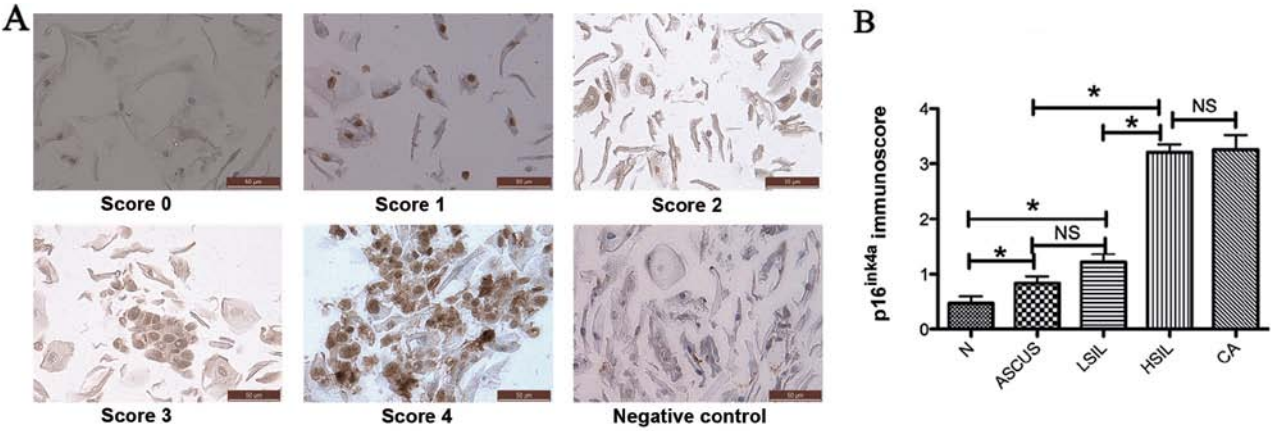


Figure 1. p16^{ink4a} is downregulated in cervical cancer cells. (A) p16^{ink4a} expression was assessed cytologically by immunocytochemistry (magnification, x400): cells with atypical cytological features were evaluated for immunoreactivity and an index of 0-4 was obtained. (B) p16^{ink4a} expression in negative cervical cells (N), atypical squamous cells of undetermined significance (ASCUS), low-grade squamous intraepithelial lesions (LSIL), high-grade squamous intraepithelial lesions (HSIL) and invasive squamous cell carcinoma (CA) was analyzed by the SNK test. *P<0.05. Bars show the means ± standard deviation (SD). NS, not significant.

Table I. Cervical cytology: p16^{ink4a} immunoscores and diagnosis of high-risk (HR)-HPV.

Pathological diagnosis	N	p16 ^{ink4a}					HPV	
		0'	1'	2'	3'	4'	Negative	Positive
ASCUS	35							
Benign lesion	25	13	12	0	0	0	10	15
CIN1	5	0	1	3	1	0	0	5
CIN2-3	5	0	0	2	3	0	0	5
LSIL	36							
Benign lesion	24	8	12	4	0	0	3	21
CIN1	5	0	2	3	0	0	0	5
CIN2-3	7	0	1	4	1	1	1	6

Benign lesion, chronic cervicitis and cervical condyloma; HPV, human papilloma virus; ASCUS, atypical squamous cells of undetermined significance; CIN, cervical intraepithelial neoplasia; LSIL, low-grade squamous intraepithelial lesion.

cases, the expression of p16^{ink4a} (P<0.05, SNK test) in cases diagnosed with CIN1 and CIN2-3 was significantly higher compared with the benign lesions. Among the LSIL cases, p16^{ink4a} (P<0.05, SNK test) expression in cases diagnosed with CIN1 and CIN2-3 was also significantly higher compared with the benign lesions. On the other hand, no significant difference was observed in the presence of high-risk (HR)-HPV (detected by the Digene test) among cases with a pathological diagnosis of CIN1, CIN2-3 and benign lesions. These results indicate a strong association between p16^{ink4a} overexpression and the development of cervical precancerous lesions. p16^{ink4a} may be particularly useful in the triage of patients with borderline smears reported as ASCUS and LSIL, suggesting

that a high p16^{ink4a} immunoreactivity correlates with a greater likelihood of progression to CIN1 and CIN2-3 lesions in the future, independent of their HPV status.

Downregulation of p16^{ink4a} inhibits cell growth. To further explore the role of p16^{ink4a} in cell proliferation and apoptosis, the cervical cancer cell lines (SiHa and HeLa) were transfected with p16^{ink4a}-siRNA. As shown in Fig. 2A and B, the mRNA and protein expression of p16^{ink4a} was decreased significantly (P<0.05). The effects of the p16^{ink4a} downregulation on cell proliferation were detected by MTT assay (Fig. 2C). MTT assay revealed that the downregulation of p16^{ink4a} markedly decreased SiHa and HeLa cell growth. We then investigated whether p16^{ink4a} is required in anchorage-dependent growth. In the SiHa and HeLa cells transfected with the p16^{ink4a}-siRNA, plate colony formation assay showed a significant decrease in the number and size of colonies compared with the cells transfected with the control-siRNA or the untreated cells (Fig. 2D and E). These findings indicate that the downregulation of p16^{ink4a} inhibits cervical cancer cell proliferation.

Downregulation of p16^{ink4a} inhibits the migration and invasion of cervical cancer cells. In order to further determine the role of the downregulation of p16^{ink4a} in cell migration, wound healing assays were performed (Fig. 3A-D). In the untreated SiHa and HeLa cells or those treated with the control-siRNA, the wound had almost closed after 12 h of incubation. However, the SiHa (P<0.001) and HeLa (P<0.05) cells treated with p16^{ink4a}-siRNA were unable to do so after 12 h of incubation. Furthermore, the results of migration and invasion assay measured in the Transwell chambers were consistent with the wound healing assay. After 10 or 24 h of incubation, migration and invasion were markedly decreased in the SiHa and HeLa cells treated with p16^{ink4a}-siRNA (Fig. 3E-H). These results suggest that the downregulation of p16^{ink4a} affects tumor metastasis in SiHa and HeLa cells.

Downregulation of p16^{ink4a} promotes apoptosis and cell cycle arrest in SiHa cells. The SiHa cells were analyzed by

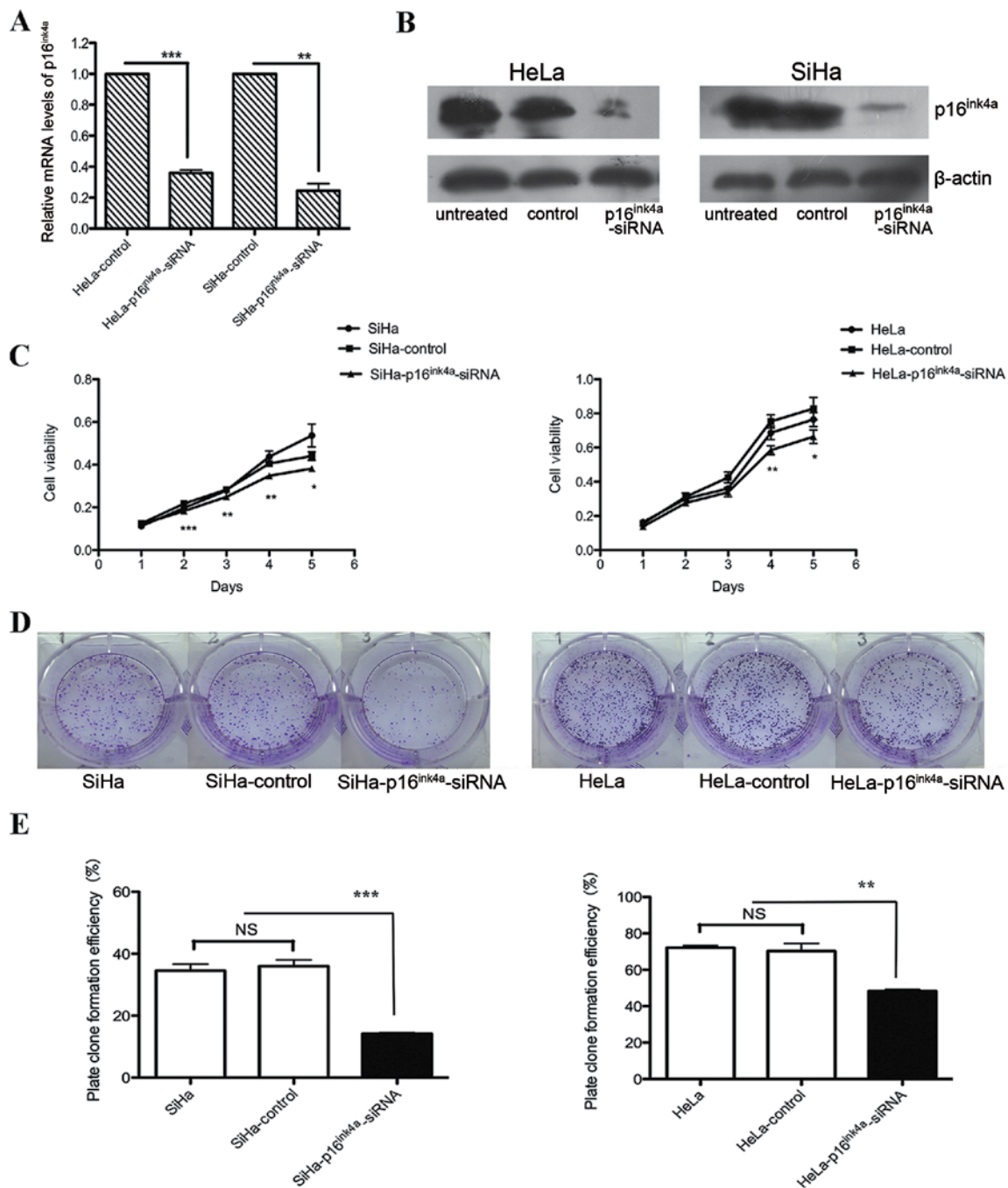


Figure 2. Downregulation of p16^{ink4a} inhibits cervical cancer cell proliferation. (A) mRNA and (B) protein expression of p16^{ink4a} in HeLa and SiHa cells was analyzed by qRT-PCR and western blot analysis, and the effectiveness of p16^{ink4a}-siRNA was confirmed by the significantly decreased p16^{ink4a} mRNA and protein expression in the HeLa and SiHa cells. (C) MTT assay was used to determine the proliferation of SiHa and HeLa cells transfected with p16^{ink4a}-siRNA or those transfected with control-siRNA and in the untreated cells. (D and E) p16^{ink4a}-siRNA also led to a significant decrease in the anchorage-dependent colony-forming ability of SiHa and HeLa cells. Untreated SiHa and HeLa cells and SiHa and HeLa cells treated with control-siRNA were used as controls. Colony formation (≥ 50 cells) was assessed using a colony counter. Columns indicate the mean number of colonies from 3 independent experiments. * $P < 0.05$, ** $P < 0.01$, *** $P < 0.001$. Bars show the means \pm standard deviation (SD). All experiments were carried out in triplicate and repeated at least 3 times. NS, not significant.

Annexin V-PI staining and flow cytometry 48 h following treatment with p16^{ink4a}-siRNA. A greater percentage of the SiHa cells transfected with p16^{ink4a}-siRNA were apoptotic, compared with those treated with the control-siRNA or the untreated group (Fig. 4A and C). The cell cycle was also determined by flow cytometry after PI staining. The results revealed that a greater number of SiHa cells transfected with p16^{ink4a}-siRNA for 48 h remained in the G1 phase,

compared with those treated with the control-siRNA or the untreated group (Fig. 4B and D). These data suggest that the downregulation of p16^{ink4a} promotes apoptosis and G1 cell cycle arrest in cervical cancer cells. To further elucidate the mechanisms of action of p16^{ink4a}, we examined the protein expression of the p16^{ink4a}-cyclin-Rb pathway in the SiHa cells transfected with p16^{ink4a}-siRNA. Western blot analysis was used to detect changes in the expression of cell cycle regu-

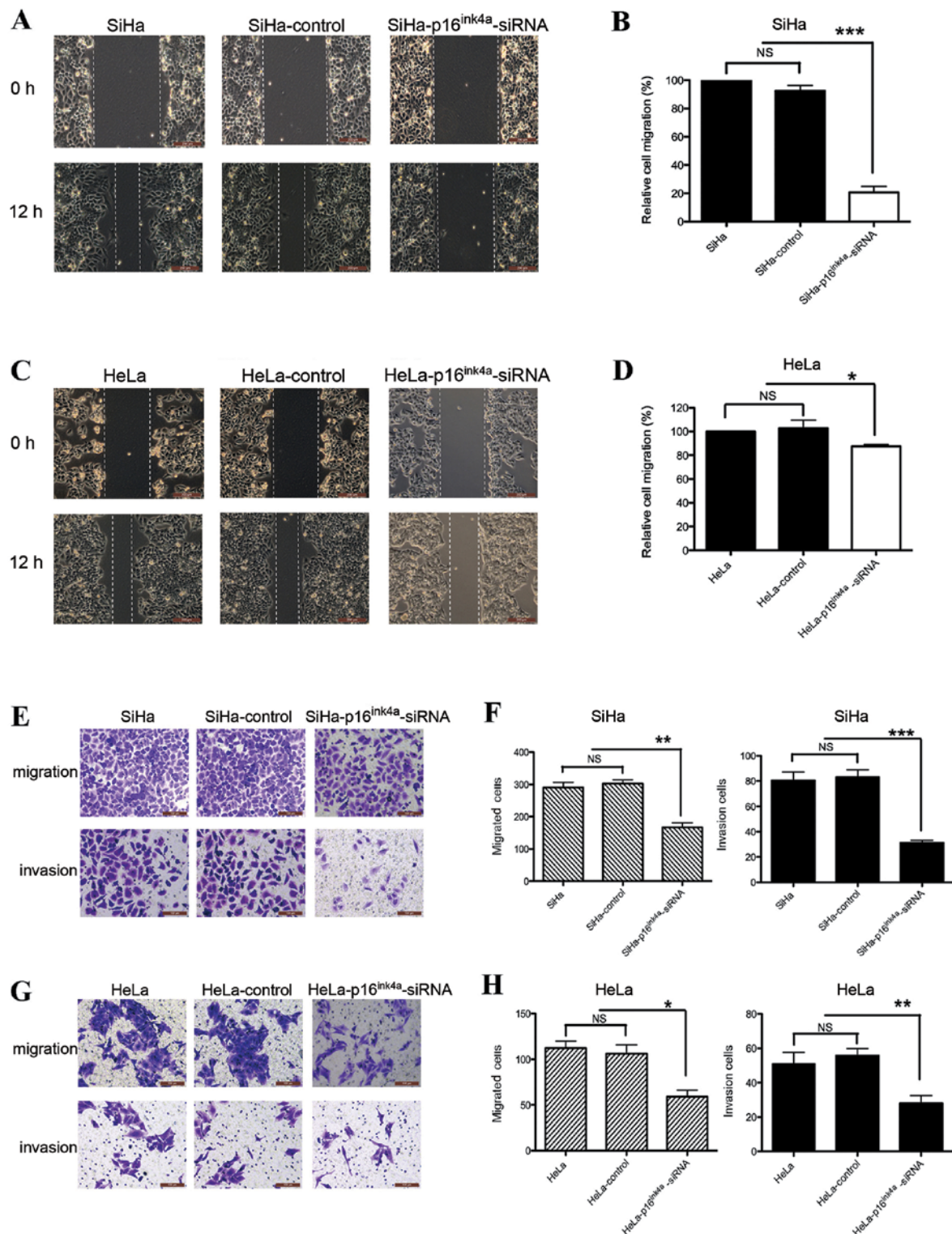


Figure 3. p16^{ink4a}-siRNA suppresses the migration and invasion ability of SiHa and HeLa cells. Wound healing assay was carried out with the (A and B) SiHa and (C and D) HeLa cells over a period of 12 h. Cells in the control group were treated with control-siRNA. Cell migration and invasion were measured in Transwell chambers (magnification, x200). Representative images are shown. Cells were counted with a microscope in 5 random high-powered fields. Migration and invasion were significantly decreased in the (E and F) p16^{ink4a}-siRNA-transfected SiHa cells and (G and H) in the p16^{ink4a}-siRNA-transfected HeLa cells. *P<0.05, **P<0.01, ***P<0.001. Bars show the means \pm standard deviation (SD). All experiments were carried out in triplicate and repeated at least 3 times. NS, not significant.

latory proteins (Fig. 4E). We found that the downregulation of p16^{ink4a} in the SiHa cells markedly induced the activation of caspase-3, a crucial mediator of programmed cell death. The expression of cyclin D1 was also decreased; however,

the levels of total Rb (tRb) and phospho-Rb protein were not significantly altered. These data suggest that the anti-tumor effects of the p16^{ink4a} downregulation are caspase-3- and cyclin D1-dependent.

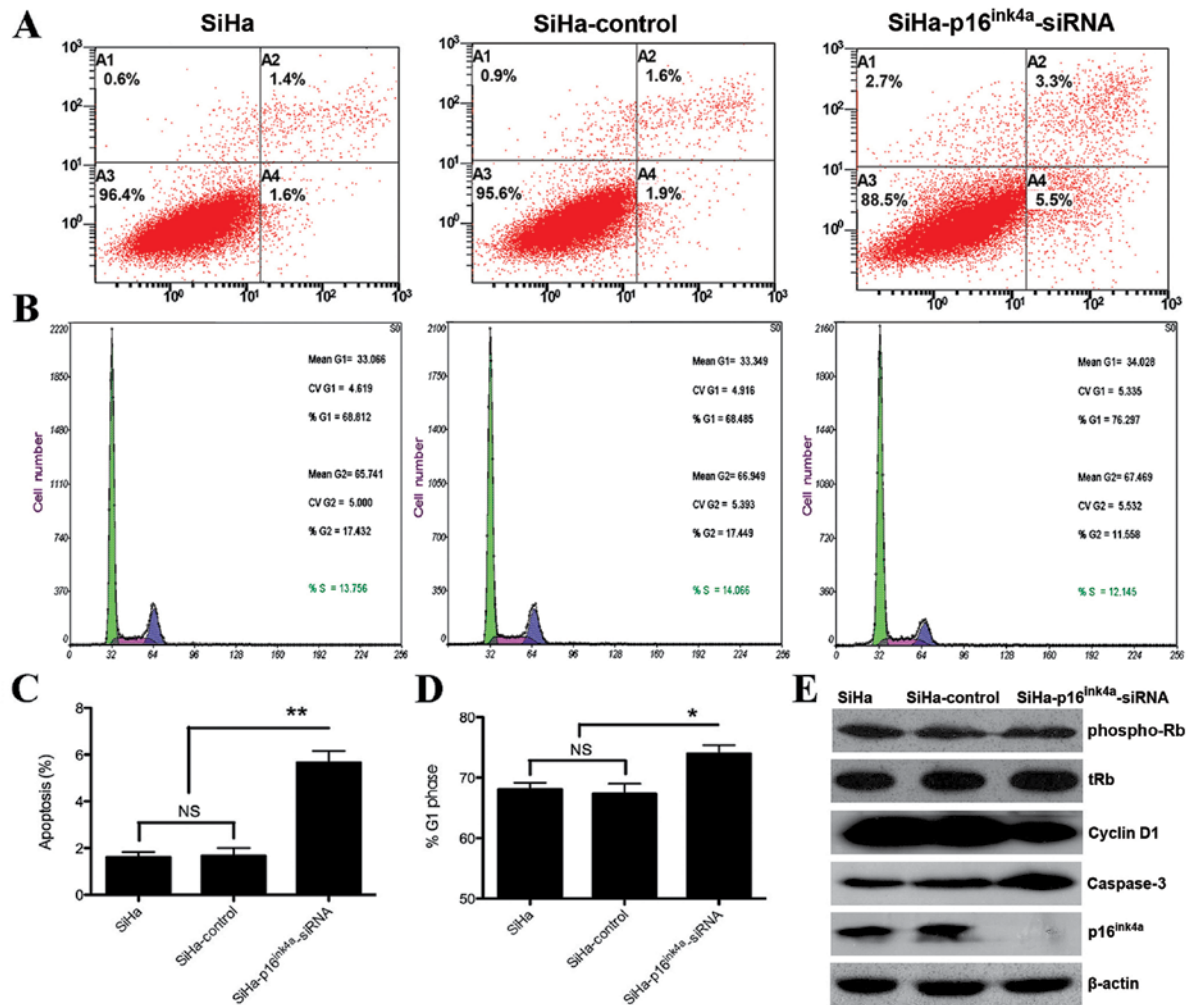


Figure 4. Downregulation of p16^{ink4a} induces apoptosis and G1 cell-cycle arrest in SiHa cells. (A and C) Representative images of flow cytometric analysis of apoptotic cells by Annexin V-propidium iodide (PI) staining in SiHa cells 48 h after transfection with p16^{ink4a}-siRNA. (B and D) Representative images of flow cytometric analysis of the cell cycle by PI staining in SiHa cells 48 h after transfection with p16^{ink4a}-siRNA; flow cytometry results were plotted as the means \pm standard deviation (SD) of triplicate experiments at 24 and 48 h after suspension culture. (E) Western blot analysis revealed a markedly higher caspase-3 expression, a decreased expression of cyclin D1 and a barely altered expression of total Rb (tRb) and phosphorylated Rb (phospho-Rb) protein levels in the SiHa cells transfected with p16^{ink4a}-siRNA. *P<0.05, **P<0.01. All experiments were carried out in triplicate and repeated at least 3 times. NS, not significant.

Discussion

Tumor dissemination and metastasis are the leading causes of death in cervical cancer. Cervical cytology screening and HPV detection are effective in the prevention of cervical cancer by identifying asymptomatic cervical cancer and its precursors. However, the screening approaches have limited sensitivity and specificity (18). In addition, no significant advances in the treatment of cervical cancer are available. It has long been recognized that p16^{ink4a}, a tumor suppressor protein, is mutated and deleted in human tumors. However, the increased p16^{ink4a} expression in cervical cancer and its precancerous lesions is associated with disorders of the negative feedback loop in the p16^{ink4a}-CDK4/6-Rb pathway of HPV-infected cells, involving E7-mediated Rb degradation (8). p16^{ink4a} immunohistochemistry in liquid-based cytology enables the detection of cancer cells and their precursors (19,20), which is consistent with our findings. Our study demonstrates that the downregulation of the overexpressed p16^{ink4a} inhibits cell proliferation and induces G1 cell cycle arrest and apoptosis in cervical cancer cell lines, suggesting that

the therapeutic targeting of the overexpressed p16^{ink4a} may be a promising treatment strategy for cervical cancer.

In the present study, we determined that the overexpression of p16^{ink4a} is associated with CIN, as p16^{ink4a} immunoreactivity was found to be higher in the HSIL and ISCC samples. Furthermore, a stronger p16^{ink4a} immunoreactivity correlated with a greater likelihood of progression to CIN1 or CIN2+ lesions in histological follow-up among the ASCUS and LSIL cases. These findings support the role of p16^{ink4a} as a potential marker in monitoring the risk of CIN1 or CIN2+ progression. We further observed that HPV DNA testing has a limited role in the clinical management of patients with ASCUS and LSIL, since most HPV infections are transient without HPV integration into the host genome. Therefore, p16^{ink4a} may be a promising marker to monitor the progression of ASCUS and LSIL and a further triage of patients.

To further explore the possible role of the overexpression of p16^{ink4a} in the progression of cervical cancer, we examined 2 cell lines derived from cervical cancer, SiHa (squamous cell carcinoma, HPV⁺) and HeLa (adenocarcinoma, HPV⁺). Cells

in which the expression of p16^{ink4a} was knocked down were established by the transfection of p16^{ink4a} siRNA into the SiHa and HeLa cells. ICC analysis suggested that the diminished p16^{ink4a} expression was associated with a lower grade of CIN and benign lesions. The downregulation of p16^{ink4a} protein expression may therefore, inhibit the progression and metastasis of cervical cancer cells.

Apoptosis plays a central role in tumor development and therapeutically-induced tumor regression. Defective apoptosis leads to the development of tumors, including cervical cancer (21,22). In this study, we found that p16^{ink4a} knock-down induced apoptosis in SiHa cells. Western blot analysis also indicated an increase in caspase-3 protein expression, suggesting that the knockdown of p16^{ink4a} may be an effective approach to delaying tumor progression. Cell cycle regulators are frequently mutated in most common malignancies. The control of cell cycle progression in cancer cells, therefore, is considered a potentially effective strategy to controlling tumor growth (23). We were surprised to find that p16^{ink4a} siRNA induced G1 cell cycle arrest with a concomitant decrease in cyclin D1 levels; however, the protein levels of tRb and phospho-Rb were only slightly altered in the SiHa cells. This observation is inconsistent with studies conducted on human glioma cell lines (24). Unlike cervical cancer, the p16^{ink4a} gene has been reported to be mutated and deleted in human glioma cell lines and glioblastoma (25,26). The suppression of the expression of p16^{ink4a} accelerates cell growth and promotes the progression of low-grade gliomas into high-grade gliomas. We suspect that such differences are partly due to the different cells used in the respective research models and HPV infection. Rb is a major protein involved in cell cycle progression from the G1 to the S phase. CDK4, CDK6 and Rb bind to the transcription factor, E2F, preventing cell cycle progression. However, the absence of any significant differences in the Rb expression level in SiHa cells transfected with p16^{ink4a}-siRNA indicated the existence of other important factors regulating the cell cycle and maintaining the stability of Rb expression in cervical cancer.

The p16^{ink4a} gene is located on chromosome 9p21. It exhibits more deletions than any other recessive cancer gene (27). It is therefore not surprising that CDK4 and its regulatory subunit, cyclin D1, which are negatively regulated by p16^{ink4a}, are embedded in the 10 most frequently amplified genomic loci in a diverse set of human cancers (28,29), such as breast and lung cancer (30,31). However, the downregulation of the overexpressed p16^{ink4a} in cervical cancer was similar to the effects of the overexpressed p16^{ink4a} in malignant gliomas (24), as regards cell proliferation and cyclin D1. Therefore, we hypothesized that p16^{ink4a} may regulate cell proliferation and apoptosis in a concentration-dependent manner, which requires further direct investigation. Despite advances in cytotoxic chemotherapy, no significant improvement has been observed in the overall survival of patients with cervical cancer. It is imperative that novel and effective treatment strategies are developed (16). The p16^{ink4a}-cyclin D1-CDK4/6-Rb protein pathway (CDK4 pathway) is dysregulated in cervical cancer, and is, therefore, an obvious therapeutic target. However, the mechanisms underlying the downregulation of p16^{ink4a} are not yet fully understood.

In conclusion, our study suggests that the overexpression of p16^{ink4a} is a prognostic indicator of cervical precancerous

lesions, and a surrogate biomarker for the diagnosis of cervical cancer. The therapeutic targeting of the overexpressed p16^{ink4a} in the p16^{ink4a}-cyclin-Rb pathway may be a promising treatment strategy for cervical cancer.

Acknowledgements

We thank Dr Huijuan Zhang and Dr Lei Pan for their help in sample collection and immunocytochemistry. This study was supported by a grant from the Project of Science and Technology Commission of Shanghai Municipality (no. 09411966900).

References

1. Jemal A, Bray F, Center MM, Ferlay J, Ward E and Forman D: Global cancer statistics. *CA Cancer J Clin* 61: 69-90, 2011.
2. Siegel R, Naishadham D and Jemal A: Cancer statistics, 2012. *CA Cancer J Clin* 62: 10-29, 2012.
3. Mayrand MH, Duarte-Franco E, Rodrigues I, *et al*: Human papillomavirus DNA versus Papanicolaou screening tests for cervical cancer. *N Engl J Med* 357: 1579-1588, 2007.
4. Gustafsson L, Pontén J, Zack M and Adami HO: International incidence rates of invasive cervical cancer after introduction of cytological screening. *Cancer Causes Control* 8: 755-763, 1997.
5. Kent A: HPV vaccination and testing. *Rev Obstet Gynecol* 3: 33-34, 2010.
6. Wang Y, Chen J, Zhang W, Hong W and Yu F: Study of the prevalence of human Papillomavirus infection in Chinese women with cervical cancer. *Afr J Microbiol Res* 6: 1048-1053, 2012.
7. Mathew A and George PS: Trends in incidence and mortality rates of squamous cell carcinoma and adenocarcinoma of cervix-worldwide. *Asian Pac J Cancer Prev* 10: 645-650, 2009.
8. Siegel R, Ward E, Brawley O and Jemal A: Cancer statistics, 2011: the impact of eliminating socioeconomic and racial disparities on premature cancer deaths. *CA Cancer J Clin* 61: 212-236, 2011.
9. Kool J, Uren AG, Martins CP, *et al*: Insertional mutagenesis in mice deficient for p15Ink4b, p16Ink4a, p21Cip1, and p27Kip1 reveals cancer gene interactions and correlations with tumor phenotypes. *Cancer Res* 70: 520-531, 2010.
10. Duan J, Chen Z, Liu P, Zhang Z and Tong T: Wild-type p16ink4a suppresses cell growth, telomerase activity and DNA repair in human breast cancer MCF-7 cells. *Int J Oncol* 24: 1597-1605, 2004.
11. Yang CT, You L, Lin YC, Lin CL, McCormick F and Jablons DM: A comparison analysis of anti-tumor efficacy of adenoviral gene replacement therapy (p14ARF and p16INK4A) in human mesothelioma cells. *Anticancer Res* 23: 33-38, 2003.
12. Wu Q, Possati L, Montesi M, *et al*: Growth arrest and suppression of tumorigenicity of bladder-carcinoma cell lines induced by the P16/CDKN2 (p16INK4A, MTS1) gene and other loci on human chromosome 9. *Int J Cancer* 65: 840-846, 1996.
13. Martin CM and O'Leary JJ: Histology of cervical intraepithelial neoplasia and the role of biomarkers. *Best Pract Res Clin Obstet Gynaecol* 25: 605-615, 2011.
14. Klaes R, Friedrich T, Spitkovsky D, *et al*: Overexpression of p16 (INK4A) as a specific marker for dysplastic and neoplastic epithelial cells of the cervix uteri. *Int J Cancer* 92: 276-284, 2001.
15. Murphy N, Ring M, Heffron CC, *et al*: p16INK4A, CDC6, and MCM5: predictive biomarkers in cervical preinvasive neoplasia and cervical cancer. *J Clin Pathol* 58: 525-534, 2005.
16. Wentzensen N, Bergeron C, Cas F, Eschenbach D, Vinokurova S and von Knebel Doeberitz M: Evaluation of a nuclear score for p16INK4a-stained cervical squamous cells in liquid-based cytology samples. *Cancer* 105: 461-467, 2005.
17. Bao W, Qiu H, Yang T, *et al*: Upregulation of TrkB promotes epithelial-mesenchymal transition and anoikis resistance in endometrial carcinoma. *PLoS One* 8: e70616, 2013.
18. Peto J, Gilham C, Fletcher O, *et al*: The cervical cancer epidemic that screening has prevented in the UK. *Lancet* 364: 249-256, 2004.
19. Cuzick J, Arbyn M, Sankaranarayanan R, *et al*: Overview of human papillomavirus-based and other novel options for cervical cancer screening in developed and developing countries. *Vaccine* 26 (Suppl 10): K29-K41, 2008.

20. Yoshida T, Fukuda T, Sano T, *et al*: Usefulness of liquidbased cytology specimens for the immunocytochemical study of p16 expression and human papillomavirus testing: a comparative study using simultaneously sampled histology materials. *Cancer* 102: 100-108, 2004.
21. Kerr JF, Wyllie AH and Currie AR: Apoptosis: a basic biological phenomenon with wide-ranging implications in tissue kinetics. *Br J Cancer* 26: 239-257, 1972.
22. Evan G and Littlewood T: A matter of life and cell death. *Science* 281: 1317-1322, 1998.
23. Molinari M: Cell cycle checkpoints and their inactivation in human cancer. *Cell Prolif* 33: 261-274, 2000.
24. Liu W, Lv G, Li Y, Li L and Wang B: Downregulation of CDKN2A and suppression of cyclin D1 gene expressions in malignant gliomas. *J Exp Clin Cancer Res* 30: 76, 2011.
25. Zadeh MD, Amini R, Firoozray M and Derakhshandeh-Peykar P: Frequent homozygous deletion of p16/CDKN2A gene in malignant gliomas of Iranian patients. *Pak J Biol Sci* 10: 4246-4250, 2007.
26. Kraus JA, Glesmann N, Beck M, *et al*: Molecular analysis of the PTEN, TP53 and CDKN2A tumor suppressor genes in long-term survivors of glioblastoma multiforme. *J Neurooncol* 48: 89-94, 2000.
27. Bignell GR, Greenman CD, Davies H, *et al*: Signatures of mutation and selection in the cancer genome. *Nature* 463: 893-898, 2010.
28. Beroukhi R, Mermel CH, Porter D, *et al*: The landscape of somatic copy-number alteration across human cancers. *Nature* 463: 899-905, 2010.
29. Anders L, Ke N, Hydbring P, Choi YJ, *et al*: A systematic screen for CDK4/6 substrates links FOXM1 phosphorylation to senescence suppression in cancer cells. *Cancer Cell* 20: 620-634, 2011.
30. Yu Q, Sicinska E, Geng Y, *et al*: Requirement for CDK4 kinase function in breast cancer. *Cancer Cell* 9: 23-32, 2006.
31. Puyol M, Martín A, Dubus P, *et al*: A synthetic lethal interaction between K-Ras oncogenes and Cdk4 unveils a therapeutic strategy for non-small cell lung carcinoma. *Cancer Cell* 18: 63-73, 2010.